Factors Influencing Curing Behavior in Phase-Separated Structures

Young Gyu Jeong, Tomoko Hashida, and Shaw Ling Hsu*

Polymer Science and Engineering Department and Material Research Science and Engineering Center, University of Massachusetts−Amherst, Amherst, Massachusetts 01003

Charles W. Paul

National Starch, Bridgewater, New Jersey 08807

Received December 6, 2004; Revised Manuscript Received January 31, 2005

ABSTRACT: Using time-resolved Fourier transform infrared spectroscopy, the reaction kinetics of ternary blends consisting of crystallizable polyester [poly(hexamethylene adipate) (PHMA)], polyether [poly(propylene glycol) (PPG)], and poly(methyl methacrylate-*co*-*n*-butyl methacrylate) [P(MMA-*co*-*n*BMA)] has been characterized. As the polyester and polyether have reactive isocyanate (NCO) units, they are able to react with water vapor in the environment. A specially designed cell was constructed to obtain reaction kinetics for samples of varying thickness at different relative humidity and temperature. Without catalysts, the reaction kinetics obtained is significantly slower than expected for the diffusion-limited mechanism of a homogeneous medium, indicating that the reaction-limited mechanism controls primarily curing in these thin films. As shown previously, the miscibility behavior of these blends at various temperatures is complex. The morphological features, which have been characterized by vibrational spectroscopy, optical microscopy, and atomic force microscopy, depend on thermal history and initial phase behavior. Reaction rates were shown to be highly dependent on sample morphology, being faster with smaller phase-separated domains and lower degrees of crystallinity.

Introduction

Isocyanate-functionalized prepolymers as moisture-curing polyurethane-based hot melt adhesives are usually reactive ternary blends consisting of a crystallizable polyester, an amorphous polyether, and a high glass transition temperature acrylate. These samples are interesting from both fundamental and practical perspectives. They are convenient to use and, once cured, exhibit very attractive physical properties.[1−4] These blends are formed by reacting macrodiols such as hydroxyl-terminated polyester and polyether with diisocyanates.[2−7] Acrylates possessing high glass transition temperature and crystallizable polyesters are included to enhance the green strength of the prepolymer in various applications. Curing is achieved by permeation of water molecules into prepolymers to react with isocyanate (NCO) groups. With the current commercial success and future potential of polyurethane-based reactive hot-melt adhesives, further understanding of the mechanism and kinetics of prepolymer curing behavior needs pursuit.

The effective reaction rate of NCO groups is an issue of great interest. As noted above, polyurethane-based reactive prepolymers are typically ternary blends. Therefore, depending on the components used, the relative composition and thermal history can affect the morphological features (phase-separated domains, degree of crystallinity, crystalline size, etc.). The spatial distribution of isocyanate groups in this complex morphology is of interest. They obviously are excluded from polyester crystalline domains. The composition distribution in the phase-separated structure needs clarification. In addition, the ability of water molecule to permeate into various regions of the prepolymers is also important in determination of the effective reactivity between NCO groups and water molecules. Last, the reaction rates between water molecules and NCO groups must be considered. These three factors will determine the ultimate reaction or curing kinetics of the prepolymers synthesized and morphologies employed. It is necessary to understand whether the overall chemical reactions are dependent on either reaction kinetics of an NCO group and water or diffusion of water molecules in the complex morphology.

As noted previously, the morphological features in these ternary blends are extremely complex.[8] The molecular weight increases, and incorporation of the urethane functional groups onto polyester and polyether greatly influences the miscibility of these ternary blends and the evolved phase-separated structures.[9] Our recent studies demonstrate that the crystallization behavior of polyesters in either the rich or poor phase is highly dependent on phase equilibria and thermal history. An extremely diverse set of samples with different degrees of crystallinity, crystallite size, and domain size can be obtained. Previous studies have determined quantitatively the effects of morphological differences on the diffusion behavior of gas- or liquid-state small molecules into polymers.[10−18] It is well accepted that permeability of small molecules, including water, decreases with increasing crystallinity. The crystallites can also reduce chain mobility in the amorphous regions. Overall, understanding morphology evolution and its features is requisite for controlling water permeability into prepolymers and curing kinetics of prepolymers.

It has recently been suggested that the curing behavior of two commercial reactive hot melt adhesives is consistent with a diffusion mechanism as described by the empirical expression[19,20]

$$z = (2VPpt)^{1/2} \quad (1)$$

* To whom correspondence should be addressed: Tel 413-577-1125; Fax 413-545-0082; e-mail slhsu@polysci.umass.edu.

10.1021/ma0474933 CCC: $30.25
Published on Web 03/08/2005

where z is cure depth, V the volume of prepolymer which reacts with 1 mol of water molecule, P the permeability coefficient of water molecules in cured prepolymer, p the water vapor pressure, and t the reaction time. This equation is based on the fact that curing proceeds with a sharp advancing front with a distinct boundary between cured and uncured prepolymer. The cured region acts as a water permeation barrier. The equation was validated by curing experiments for thick samples in the order of millimeters. The change of cure depth (z) with $t^{1/2}$ shows good linearity at various relative humidity conditions,[20] thus indicating that diffusion-limited mechanism controls moisture-curing of reactive hot melt adhesives. It was also reported that one sample cures more rapidly than another due to its lower crystallinity.

There was, however, no discussion related to curing behavior of prepolymers based on material factors such as components used, composition, miscibility, etc. The effects of temperature and relative humidity were not discussed. As prepolymer is usually applied to various substrates with dozens or hundreds of micrometers thickness, the curing behavior of prepolymers in thin sample dimension also needs to be investigated. The curing kinetics and mechanism in thin sample dimension may differ from bulk samples with significant cured regions. Last, because of the various accelerators used in commercial formulations, their effects on the reaction kinetics may not correspond to the reactivity kinetics reported for NCO group and water.[21]

The present study addressed primarily the effects of sample thickness, temperature, relative humidity, and morphological features (crystalline domain size and crystallinity) on the curing behavior of reactive ternary prepolymers. Various morphologies of typical model prepolymer were prepared. Time-resolved Fourier transform infrared spectroscopy utilized a custom-designed cell to monitor curing behavior of prepolymer in thin films. Crystallization kinetics and morphological features developed were investigated using infrared spectroscopy, optical microscopy, and atomic force spectroscopy. Laser confocal Raman spectroscopy was used to characterize compositional distribution. In this study, we eliminated all effects from the presence of catalysts. The mechanism and kinetics of prepolymer curing in these thin samples have been addressed.

Experimental Section

Prepolymer Synthesis and Characterization. Crystalline poly(hexamethylene adipate) (PHMA), amorphous poly(propylene glycol) (PPG), and amorphous poly(methyl methacrylate-*co*-*n*-butyl methacrylate) [P(MMA-*co*-*n*BMA)] copolymer with high glass transition temperature were mixed to form reactive ternary blends. PHMA was obtained from Dow Chemical (M_n = 1600 g/mol, M_w/M_n = 1.59, T_m = 55 °C, T_g = −61 °C, and hydroxyl value = 46). PPG was obtained from ARCH Chemical (M_n = 1900 g/mol, M_w/M_n = 1.01, T_m = −30 °C, T_g = −66 °C, and hydroxyl value = 56). P(MMA-*co*-*n*BMA) random copolymer was obtained from INEOS Acrylics (M_n = 18 800 g/mol, M_w/M_n = 1.64, and T_g = 85 °C). Methylene bis(phenyl isocyanate) (MDI) (Aldrich, 98.0%) was used as received. Chemical structures of these materials are presented in Figure 1.

PHMA and PPG, with the exception of P(MMA-*co*-*n*BMA), have hydroxyl (OH) groups at their chain ends which react with NCO groups of MDI during prepolymer synthesis. On the basis of previously established phase diagrams,[8] we selected a representative composition of PHMA/PPG/P(MMA-*co*-*n*BMA) to be 36/36/29 wt %. As in our previous studies, the amount of

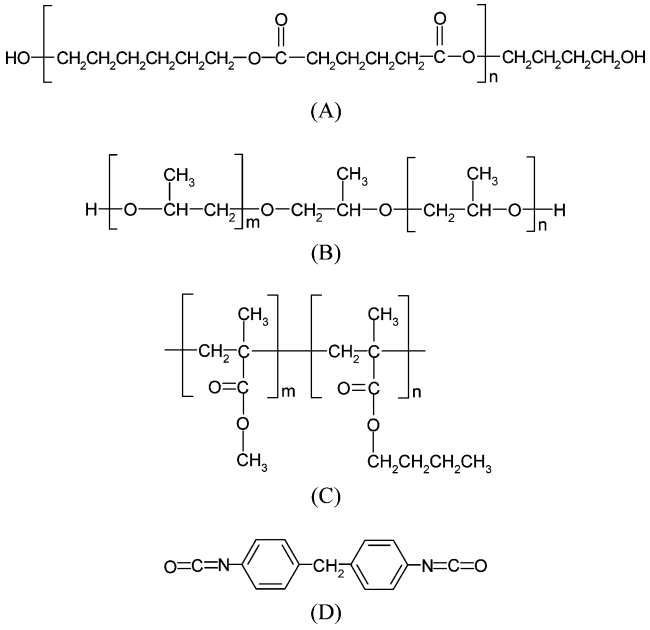

Figure 1. Chemical structures of prepolymer components: (A) PHMA; (B) PPG; (C) P(MMA-*co*-*n*BMA); (D) MDI.

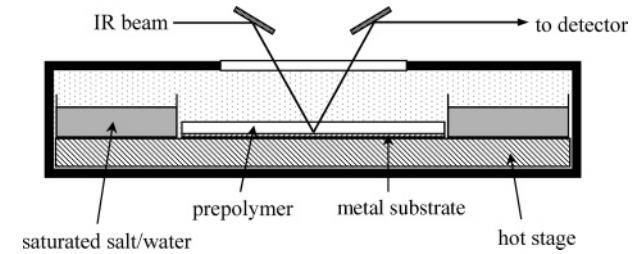

Figure 2. Custom-designed cell built with well-controlled temperature and relative humidity. Time-resolved infrared spectra were obtained in the reflectance mode to monitor the curing behavior of prepolymers.

MDI was kept as [NCO]/[OH] = 1.68.[22] Before use, PPG, PHMA, and P(MMA-*co*-*n*BMA) were predried in a reactor under high vacuum in a two-step process (60 °C for 24 h and 120 °C for 2 h) to eliminate moisture. Subsequently, prepolymers were prepared by reacting MDI with PPG and PHMA under vacuum at 120 °C for 3 h. Prepolymers were then kept under nitrogen at room temperature to minimize further reaction of NCO groups. Some synthesized prepolymers were terminated with methanol to prevent further chemical reaction of NCO groups. These were used for ^{1}H NMR characterization and studies of crystallization kinetics. ^{1}H NMR was used to determine the relative percentage of NCO groups that participate in urethane and allophanate formation. For the 36/36/29 prepolymer synthesized, it was found that ca. 30% of NCO group of MDI remain unreacted. Under these conditions, the amount of allophanate formed is negligible.[22] A detailed ^{1}H NMR prepolymer analysis has been presented previously.[22]

Reflection−Absorption Infrared (RA-IR) Spectroscopy. Time-resolved reflectance infrared spectroscopy was undertaken to monitor curing behavior of prepolymer film with thickness in the order of microns. The incidence angle was kept at 30°. Cleaned steel sheets of 0.1 mm thickness were used as substrate. Unless otherwise specified, prepolymers with 20 μm thickness were applied on the substrate. A custom-designed experimental cell, shown in Figure 2, controlled reaction temperature and relative humidity. This cell was accommodated in a Perkin-Elmer 2000 FT-IR spectrometer. The relative humidity was controlled using a saturated water/salt reservoir.[23] The salts used are $MgCl_2$ and K_2SO_4. Prior to the curing experiments, the relative humidity in the experimental setup was calibrated by changing temperature from 25 to 65 °C for a given saturated salt solution. With increasing tem-

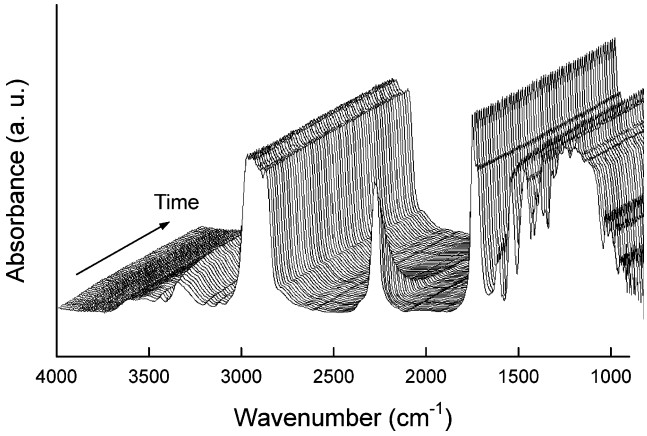

Figure 3. Time-resolved reflectance infrared spectra for the 36/36/29 prepolymer at a curing condition of 25 °C and 94% RH.

perature from 25 to 65 °C, the relative humidity decreased 32 to 24% for $MgCl_2$/water and 94 to 62% for K_2SO_4/water.

In the curing experiments, the synthesized prepolymer was first applied to the steel substrate at 120 °C for 3 min in a glovebox purged with N_2 gas. It was then transferred rapidly to our custom-designed cell set at a predetermined temperature and relative humidity. Subsequently, the curing reaction was monitored by obtaining RA-IR spectra as a function of time. A new spectrum was acquired every 3 min. Spectral resolution was typically set to 2 cm^{-1}. The signal-to-noise ratio obtained is quite good and adequate for our analysis, as can be seen in Figure 3. Absorbance of the CH stretch band due to methyl and methylene groups from 3100 to 2700 cm^{-1} remains unchanged through the curing reaction and used as internal calibration. Absorbance of the asymmetric NCO stretch band from 2450 to 2150 cm^{-1} decreases significantly with reaction time, confirming the fact that NCO groups are the dominant functional groups involved in curing reactions triggered by water molecule permeation into prepolymer.

Time-resolved infrared spectroscopy was used to investigate the morphology evolution (crystallization kinetics and relative crystallinity) of prepolymer at various crystallization temperatures from 25 to 45 °C. In this case, an inactive prepolymer terminated with methanol was used to prevent unintended curing reactions. The degree of crystallinity in these samples can be measured using the normalized intensities of infrared-active bands. The skeletal deformation band at 971 cm^{-1} has been shown to be directly associated with the ordered chain conformation in the crystalline state. Since the melting enthalpy of PHMA is known,[24] calorimetric measurements of these blends can then be used to calibrate the intensity of the 971 cm^{-1} band. The degree of crystallinity of samples prepared under different experimental conditions can be measured using infrared experiments.

Laser Confocal Raman Spectroscopy. Laser confocal Raman spectroscopy (LabRam HR800 Raman microscope, Jobin Yvon Co.) was used to characterize the compositional distribution in the prepolymer with phase-separated morphology. This instrument can achieve a spatial resolution of ~1 μm^2 area. The spectral resolution was kept at 1 cm^{-1}. Raman spectra of polymer components of PHMA, PPG, P(MMA-*co*-*n*BMA), and inactive MDI terminated with methanol were obtained for comparison.

Optical Microscopy. Optical morphology of prepolymers was observed using an Olympus Vanox optical microscope with a hot stage and digital camera (Kodak EASYSHARE LS443). Specimens were prepared by melting the prepolymer between two glass slides on a hot stage at 120 °C for 3 min under N_2 gas atmosphere to minimize chemical reactions during experiments. Optical micrographs of the prepolymer were recorded by controlling temperature from 120 to 20 °C to characterize morphological features such as liquid/liquid phase separation and crystallization.

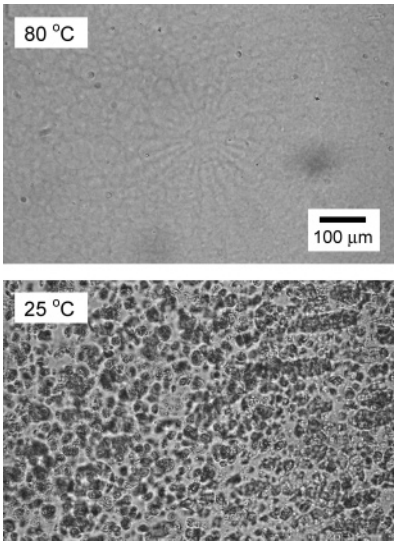

Figure 4. Optical micrographs of the 36/36/29 prepolymer at 80 and 25 °C.

Atomic Force Microscopy (AFM). Surface morphology of prepolymers with different thermal history was characterized using a Digital Instruments Dimension TM300 scanning force microscope in the tapping mode. AFM images were obtained in both height and phase contrast modes. The areas scanned were 10 × 10 μm^2.

Results and Discussion

Prepolymer Morphology and Compositional Distribution. Prepolymer morphology can be quite complex and varies considerably depending on composition and thermal history.[8,9] One component is crystallizable polyester. Polyether and acrylate are amorphous components with low and high glass transition temperatures, respectively. Figure 4 shows optical micrographs of observed prepolymer morphologies. The heterogeneous phase-separated morphology observed at room temperature for all ternary blends undoubtedly originates from differences in crystallization behavior of polyester in the polyester-rich and polyester-poor regions. The phase-separated domain size was also observed to be dependent on temperature and time.

For the 36/36/29 prepolymer displaying liquid/liquid phase-separated morphology, laser confocal Raman spectra were obtained from domains and matrix to characterize compositional distribution, as shown in Figure 5. Raman spectra of individual components such as PHMA, PPG, P(MMA-*co*-*n*BMA), and inactive MDI were also obtained. On the basis of the characteristic signature of each component, it is evident that PHMA (1087 and 1420 cm^{-1}) is the predominant component in the domains and P(MMA-*co*-*n*BMA) (600 and 812 cm^{-1}) and PPG (1342 cm^{-1}) are more predominant in the continuous matrix. The domain and matrix in the phase-separated morphology are therefore concluded to be PHMA-rich and PHMA-poor, respectively. These Raman spectral results match well with morphological observations using optical microscopy.

As discussed in the Introduction, distribution of prepolymer components, including NCO groups in the phase-separated morphology, is essential in consideration of curing kinetics. In the phase-separated morphology, water molecule permeability and reactivity differ in each region. Thus, the overall curing rates initiated by the reaction between NCO groups and

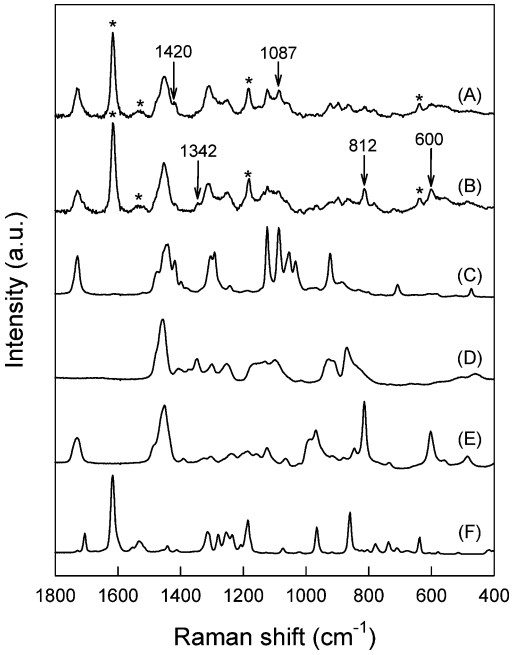

Figure 5. Raman spectra from the phase-separated domain and matrix of the 36/36/29 prepolymer and of prepolymer components: (A) domain (PHMA-rich phase); (B) matrix (PHMA-poor phase); (C) PHMA; (D) PPG; (E) P(MMA-*co*-*n*BMA); (F) inactive MDI. The asterisks at 637, 1182, 1530, and 1616 cm^{-1} indicate Raman peaks from inactive MDI.

permeating water molecules should be dependent on the accessibility of the reactive groups. Raman intensities of MDI at 637, 1182, 1530, and 1616 cm^{-1}, marked with asterisks in Figure 5, were found to be quite similar in intensity (~10%) within the spatial resolution measurable (~1 μm^2) for all regions. This suggests that the NCO functional groups at the ~1 μm^2 spatial resolution are homogeneously distributed. If fully reacted, both PHMA and PPG are terminated with reactive NCO groups. Because polyester and polyether have similar molecular weight, the similarity of MDI content in the two phases appears reasonable at the ~1 μm^2 spatial resolution employed.

Curing Mechanism in Thin Prepolymer Film. As mentioned above, the prepolymer curing is achieved by permeation of water molecules into prepolymer and the chemical reactions initiated by the reaction between NCO groups and water molecules. It is interesting to consider the role of water diffusion vs reaction kinetics in the analysis of overall curing rates. If the water molecule permeability is dominant in comparison to the reaction rates, prepolymer curing is controlled by the permeation rate of water molecules into prepolymer, as described by eq 1. If curing is controlled by the reaction rates of the functional groups involved, one can consider that water molecules permeate into prepolymers prior to reaction, and the overall reaction kinetics can be expressed as

$$-\frac{d[NCO]}{dt} = k[NCO][H_2O] \tag{2}$$

where [NCO] and [H_2O] are the concentrations of NCO and water molecules, respectively. k is the rate constant which is expressed with Arrhenius-type temperature dependence

$$k = A \exp\left(\frac{-E_a}{RT}\right) \tag{3}$$

where A is the frequency factor, E_a the activation energy, R the gas constant, and T the reaction temperature. In the pure reaction-limited mechanism, [H_2O] of eq 2 is constant.

The influence of sample thickness on prepolymer curing was investigated using the 36/36/29 prepolymer with sample thickness ranging from 5 to 80 μm. The change of NCO group concentration measured by infrared spectroscopy with respect to time was taken to be representative of the curing kinetics. The conversion, p_{NCO}, of NCO groups is defined as follows

$$p_{NCO} = \frac{A_t}{A_0} \tag{4}$$

where A_t and A_0 are the integrated absorbance of the NCO stretch band as a function of time, t, and at zero reaction time, respectively. The integrated absorbance (A_0) of the NCO stretch band at $t = 0$ exhibits linear behavior as a function of thickness, as shown in Figure 6A. This result illustrates that infrared spectra are representative of the entire sample, and the data are characteristic of curing behavior throughout the film. In Figure 6B, the changes of A_t with t exhibit a typical exponential decay of chemical reaction kinetics. In Figure 6C, the changes of A_t with $t^{1/2}$ show evidence of linearity in the intermediate region. As noted above, the integrated absorbance (A_0) at zero reaction time is linearly proportional to sample thickness. Therefore, if prepolymer curing is achieved by the diffusion-limited mechanism of eq 1, changes of A_t with $t^{1/2}$, shown in Figure 6C, are considered the same as those of the cured depth (z) with $t^{1/2}$ and that the slopes, $(2VPp)^{1/2}$, should be constant, regardless of sample thickness. However, the slopes increase from 8.71 to 54.42 $\mu m/h^{1/2}$ with increasing sample thickness from 5 to 80 μm. In addition, the values are much lower by one order in comparison to reported values.[20] These results indicate that curing of prepolymer with dozens of micrometers thickness is not dominated by the diffusion-limited mechanism.

It was reported that the E_a of eq 3 for the reaction between the phenyl isocyanate and water molecules in dioxane is 45.98 kJ/mol.[21] We therefore conclude that prepolymer curing in thin films is mostly controlled by the reaction rates rather than diffusion rate. When the conversion of NCO groups (p_{NCO}) is represented as a function of time, as shown in Figure 6D, all plots do not, however, exactly overlap. The curves shift along the time axis with increasing sample thickness. Curing takes longer for thicker samples, indicative of some diffusion contributions. This results from the fact that [H_2O] of eq 2 changes with reaction time due to the time dependence of water molecule permeation. We note again that our samples do not have catalysts, whose role on effective reaction kinetics will be discussed in another paper.

Effects of Temperature and Relative Humidity on Prepolymer Curing. Using the 36/36/29 prepolymer as an example, curing experiment was conducted at various temperatures and relative humidity. The results are plotted in Figure 7. As expected, at the same temperature, curing rates are faster at higher relative humidity due to the increased [H_2O] of eq 2. In addition,

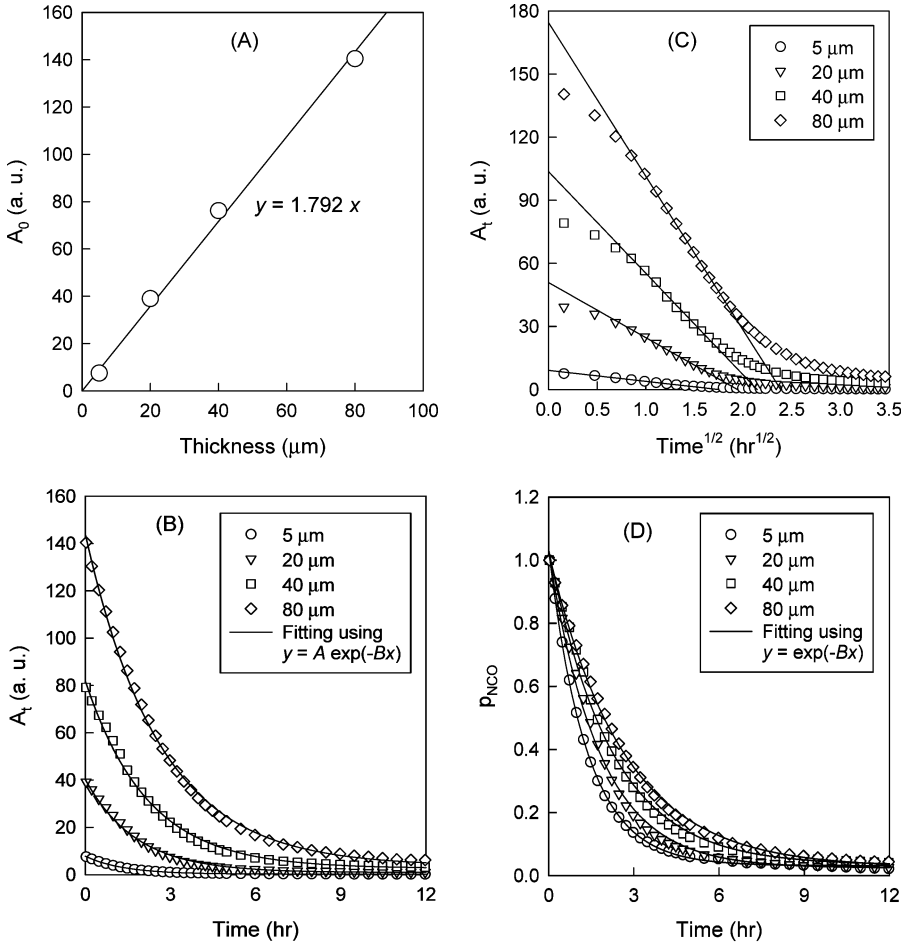

Figure 6. (A) Integrated absorbance (A_0) of NCO group at zero reaction time for the 36/36/29 prepolymer samples with various sample thickness. (B) Changes of absorbance of NCO group (A_t) as a function of time at 25 °C and 94% RH. (C) Changes of absorbance of NCO group (A_t) as a function of square root of time ($t^{1/2}$). (D) Conversions of NCO group (p_{NCO}) as a function of time. In (B) and (D), A and B of $y = A \exp(-Bx)$ are parameters to fit the data.

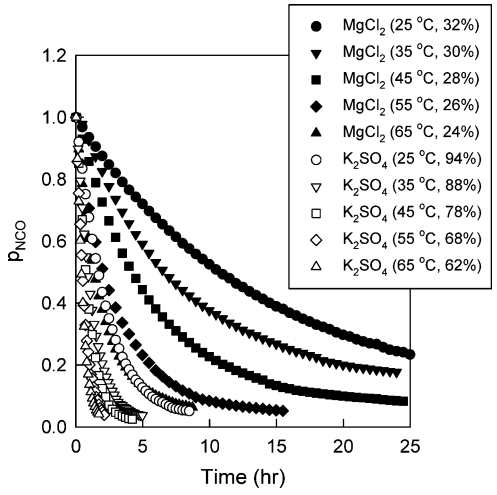

Figure 7. Conversions of NCO group (p_{NCO}) as a function of time for the 36/36/29 prepolymer samples at various curing conditions.

the rate constant (k) of eqs 2 and 3 increases with increasing the ratio of $[H_2O]/[NCO]$.[21] It was also observed that the curing rate of the prepolymer increases with increasing the temperature from 25 to 65 °C. The increase in curing dynamics with increasing temperature is partially due to the increased vapor pressure (p).[23] The vapor pressure of pure water (p_0) increases from 3.17 to 25.02 kPa with increasing the temperature from 25 to 65 °C.[23] In the same temperature range, the vapor pressure of the saturated salt solutions is increased from 1.02 to 6.03 kPa for $MgCl_2$/water and 2.98 to 15.39 kPa for K_2SO_4/water. Chain mobility must also increase at elevated temperatures. Since the polyester in this ternary blend has a melting temperature ranging from 50 to 55 °C, the degree of crystallinity must have been lowered at elevated temperatures. Both factors contribute to the accessibility and reactivity of water molecules to NCO groups.

Morphology Evolution and Its Effect on Curing. It is our hypothesis that the macroscopic phase-separated structures and the degree of crystallinity can both affect curing behavior. The morphological features of prepolymers are strongly dependent on thermal history. The 36/36/29 prepolymer exhibits a liquid/liquid phase separation. Two samples, A and B, with different thermal history were prepared to obtain samples of different domain size but similar degree of crystallinity. Both samples were first heated at 120 °C for 3 min. Subsequently, sample A was crystallized at 25 °C after annealing at 65 °C for 10 h. Sample B was crystallized directly at 25 °C for 10 h without the intermediate annealing step. Sample preparation was carried out in a glovebox purged with N_2 gas in order to eliminate any possibility of curing from ambient water molecules. Curing experiments were carried out at 25 °C and 32% RH. The curing rate of sample A was found to be much slower than sample B, as shown in Figure 8.

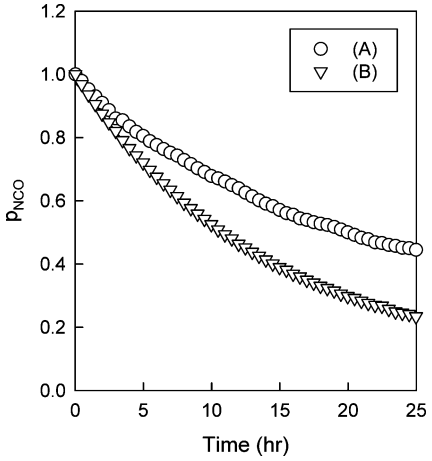

Figure 8. Conversions of NCO group (p_{NCO}) as a function of time at a curing condition of 25 °C and 32% RH for the 36/36/29 prepolymer samples with different thermal history: (A) crystallized at 25 °C after annealing at 65 °C for 10 h; (B) crystallized at 25 °C for 10 h without annealing.

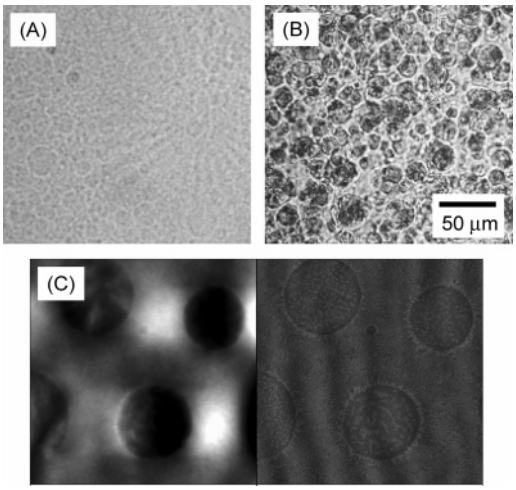

Figure 9. (A) Optical micrograph of the 36/36/29 prepolymer (sample A) annealed at 65 °C for 10 h. (B) Optical micrograph of sample A crystallized at 25 °C after annealing at 65 °C for 10 h. (C) AFM images of sample A crystallized at 25 °C after annealing at 65 °C for 10 h. The AFM image from the left-hand side is height-contrast and phase-contrast image, respectively. The image size is 10 × 10 μm^2.

The bulk and surface morphology of samples A and B were characterized using optical microscopy and AFM. The size of the PHMA-rich domains in sample A was found to be much larger than that of sample B, as shown in Figures 9 and 10. As noted above, this 36/36/29 prepolymer displays liquid/liquid phase separation above its melting temperature of ca. 50 °C. The domain of the phase-separated morphology is associated with a PHMA-rich phase. The larger domain size of sample A results from increasing chain mobility maintained at elevated temperatures, characteristic of annealing behavior. As shown in Figures 9 and 10, the PHMA-rich domain size of sample A is 10−30 times larger than that of sample B. Water molecule permeability in the crystalline PHMA-rich domain is slower than in the matrix. As the PHMA-rich domain size increases, water permeation is slower, and thus the reactivity of NCO groups with the permeating water molecules is retarded, thus lowering the curing rate in sample A in comparison to sample B. It should be noted that the degree of crystallinity

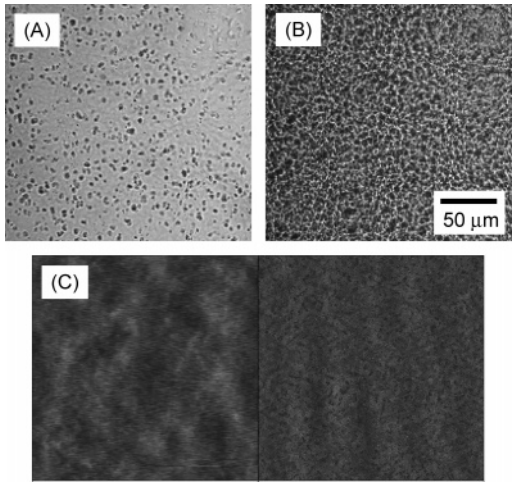

Figure 10. (A) Optical micrograph of the 36/36/29 prepolymer (sample B) at initial crystallization at 25 °C. (B) Optical micrograph of sample B crystallized at 25 °C for 10 h without annealing. (C) AFM images of sample B crystallized at 25 °C for 10 h without annealing. The AFM image from left-hand side is height-contrast and phase-contrast image, respectively. The image size is 10 × 10 μm^2.

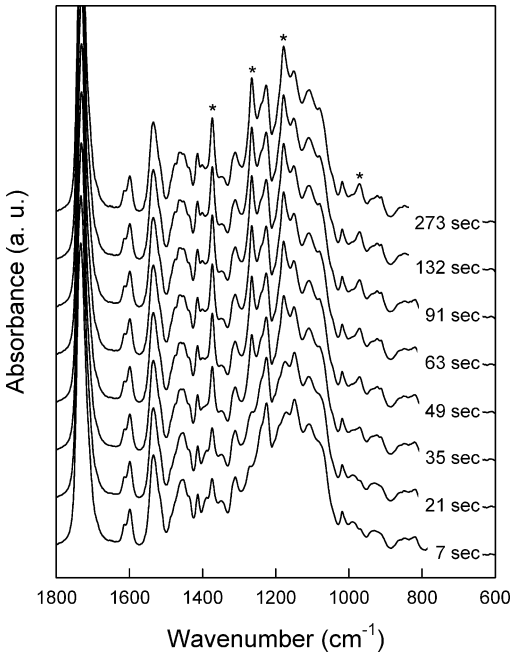

Figure 11. Time-resolved infrared spectra for the 36/36/29 prepolymer sample crystallizing at 25 °C. The asterisks at 971, 1178, 1267, and 1374 cm^{-1} indicate the crystalline PHMA bands.

measured by DSC are 13.1 and 12.4% for samples A and B, respectively.

Crystalline features associated with polyesters within individual domains should also be considered in analysis of reaction kinetics between NCO groups and water molecules. Water molecules must necessarily migrate around crystalline regions to react with accessible NCO groups. As shown above, the differing domain size is important. The degree of crystallinity within domains is equally important. Crystallinity can be followed using infrared spectroscopy. For the inactive 36/36/29 prepolymer terminated with methanol, infrared spectra obtained as a function of time during crystallization at 25 °C are shown in Figure 11. The crystalline bands at 971, 1178, 1267, and 1374 cm^{-1} noticeably increase with

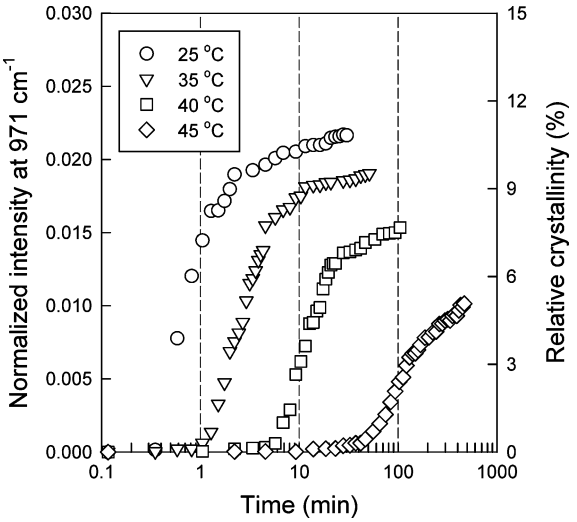

Figure 12. Relative crystallinity development as a function of time for the inactive 36/36/29 prepolymer terminated with methanol at various crystallization temperatures. The normalized absorbance at 971 cm^{-1}, evaluated from time-resolved infrared spectra, was used to evaluate the relative crystallinity.

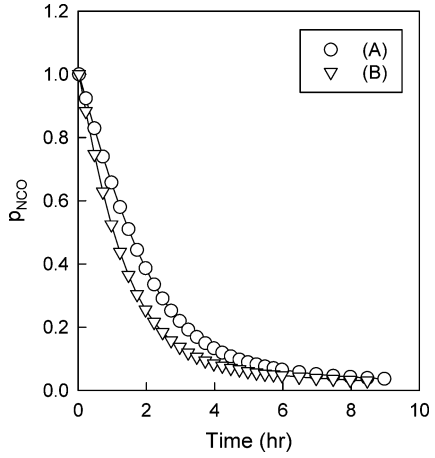

Figure 13. Conversions of NCO group (p_{NCO}) as a function of time at 25 °C and 94% RH for the 36/36/29 prepolymer samples with different relative crystallinity: (A) crystallized at 25 °C for 3 h; (B) crystallized at 45 °C for 3 h.

time. Of the crystalline PHMA bands, the normalized integrated absorption (using the CH stretching region as reference) of the 971 cm^{-1} band was analyzed. The evolution of the degree of crystallinity at various crystallization temperatures from 25 to 45 °C is shown in Figure 12. As supercooling decreases, the crystallization rate decreases and relative crystallinity is also suppressed. At all temperatures, crystallization behavior exhibits three steps, i.e., induction period, onset of crystallization, and prior to reaching a plateau. Induction time increases with increasing crystallization temperature or lower supercooling. As for all crystallization processes associated with polymers, the degree of crystallinity is highly dependent on crystallization temperature and time.

Two samples with different crystallinity were prepared to investigate the influence of crystallinity on curing kinetics. The 36/36/29 prepolymer samples were melted at 120 °C and then crystallized at 25 and 45 °C for 3 h. Curing kinetics study of each sample was carried out at 25 °C and 94% RH, as shown in Figure 13. The sample crystallized at 25 °C for 3 h displayed a slower curing rate than the sample crystallized at 45 °C. The

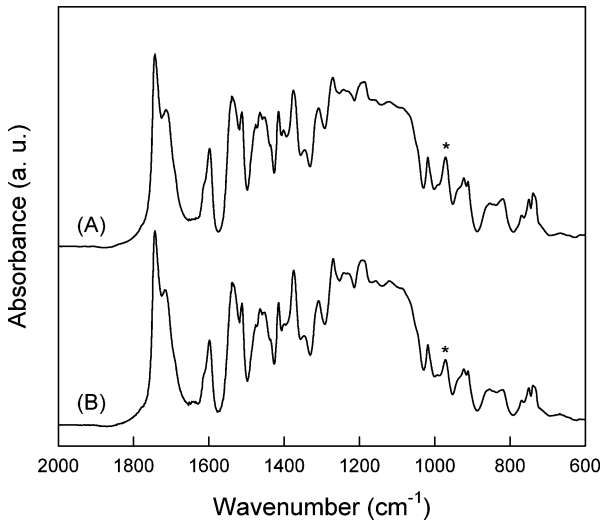

Figure 14. Infrared spectra after curing at 25 °C and 94% for the 36/36/29 prepolymer samples with different crystallinity: (A) crystallized at 25 °C for 3 h; (B) crystallized at 45 °C for 3 h.

relative crystallinity between the two samples was compared using the integrated absorbance at 971 cm^{-1} of the infrared spectra shown in Figure 14. The sample crystallized at 25 °C (degree of crystallinity, 11.9%) was found to have nearly twice as high crystallinity as compared to the sample crystallized at 45 °C (degree of crystallinity, 5.3%). Therefore, it is concluded that the slow curing rate of the sample crystallized at 25 °C is due to its higher degree of crystallinity. The crystallites serve as impediments to the mobility and reactivity of water molecules. The NCO groups are too large to fit into the crystalline regions and thus segregate into amorphous regions. Our data indicate that an increase in the degree of crystallinity results in a decrease in reaction kinetics. Morphological features such as degree of crystallinity and PHMA-rich domain size cause substantial differences in curing behavior of prepolymers. In our case, it is clear that without catalysts the determining factor is the low reaction rate between NCO groups and water molecules. Nevertheless, morphological features are also influential. Therefore, both reaction kinetics and molecular diffusion contribute to the overall curing kinetics.

Conclusions

This study involved synthesis of model reactive 36/36/29 prepolymer with considerably different morphological features due to liquid/liquid phase separation and crystallization. The phase-separated structure and degree of crystallinity were altered by controlling crystallization conditions. The curing kinetics of the prepolymer was investigated as a function of sample thickness, temperature, and relative humidity. Thin samples can be studied with reflectance infrared spectroscopy. Laser confocal Raman spectroscopy, optical microscopy, and atomic force microscopy were utilized to study morphological features. The degree of crystallinity was measured on the basis of infrared-active crystalline bands. NCO functional groups, which react with permeating water molecules, were found distributed homogeneously, even in phase-separated morphology. Curing rates of prepolymers was mostly dominated by the reaction-limited rather than diffusion-limited mechanism. In addition, prepolymer curing was found to be faster with

increased temperature and/or humidity due to enhanced vapor pressure (increased water molecules concentration, mobility, and reactivity). For the 36/36/29 prepolymer, morphological features such as polyester-rich domain size and degree of crystallinity, which are sensitive to thermal history, were found to noticeably affect prepolymer curing rates. Increasing domain size and crystallinity, due to the decreased accessibility and reactivity of water molecules, retards curing rates.

Acknowledgment. The authors thank the National Science Foundation-Environment Protection Agency (TSE Grant # RD831636010) for their financial support. We also appreciate a grant from National Starch, a subsidiary of ICI, for supporting this research.

References and Notes

(1) de Genova, R.; Grier, L.; Murray, P.; Clay, W. *Tappi J.* **1998**, *6*, 196.
(2) Vick, C. B.; Okkonen, E. A. *For. Prod. J.* **1998**, *48*, 71.
(3) Szycher, M. *Szycher's Handbook of Polyurethanes*; CRC Press: Boca Raton, FL, 1999.
(4) Forschner, T. C.; Gwyn, D. E.; Xiao, H. X.; Suthar, B.; Sun, L. Q.; Frisch, K. C. *Adhes. Age* **1999**, *42*, 20.
(5) Thompson, C. M.; Taylor, S. G.; McGee, W. W. *J. Polym. Sci., Part A: Polym. Chem.* **1990**, *28*, 333.
(6) Lepene, B. S.; Long, T. E.; Meyer, A.; Kranbuehl, D. E. *J. Adhes.* **2002**, *78*, 297.
(7) Cui, Y. J.; Hong, L.; Wang, X. L.; Tang, X. Z. *J. Appl. Polym. Sci.* **2003**, *89*, 2708.
(8) Duffy, D. J.; Stidham, H. D.; Hsu, S. L.; Sasaki, S.; Takahara, A.; Kajiyama, T. *J. Mater. Sci.* **2002**, *37*, 4851.
(9) Duffy, D. J.; Heintz, A. M.; Stidham, H. D.; Hsu, S. L.; Suen, W.; Chu, W.; Paul, C. W. *J. Adhes.* **2003**, *79*, 1091.
(10) Kreituss, A.; Frisch, H. L. *J. Polym. Sci., Part B: Polym. Phys.* **1981**, *19*, 889.
(11) Perrin, L.; Nguyen, Q. T.; Clement, R.; Neel, J. *Polym. Int.* **1996**, *39*, 251.
(12) Horas, J. A.; Rizzotto, M. G. *J. Polym. Sci., Part B: Polym. Phys.* **1996**, *34*, 1541.
(13) Horas, J. A.; Rizzotto, M. G. *J. Polym. Sci., Part B: Polym. Phys.* **1996**, *34*, 1547.
(14) Hedenqvist, M.; Gedde, U. W. *Prog. Polym. Sci.* **1996**, *21*, 299.
(15) Horas, J. A.; Rizzotto, M. G. *Polym. Eng. Sci.* **1999**, *39*, 1389.
(16) Sekelik, D. J.; Stepanov, E. V.; Nazarenko, S.; Schiraldi, D.; Hiltner, A.; Baer, E. *J. Polym. Sci., Part B: Polym. Phys.* **1999**, *37*, 847.
(17) Sammon, C.; Yarwood, J.; Everall, N. *Polymer* **2000**, *41*, 2521.
(18) McGonigle, E. A.; Liggat, J. J.; Pethrick, R. A.; Jenkins, S. D.; Daly, J. H.; Hayward, D. *Polymer* **2001**, *42*, 2413.
(19) Comyn, J.; Day, J.; Shaw, S. J. *J. Adhes.* **1998**, *66*, 289.
(20) Comyn, J.; Brady, F.; Dust, R. A.; Graham, M.; Haward, A. *Int. J. Adhes. Adhes.* **1998**, *18*, 51.
(21) Saunders, J. H.; Frisch, K. C. *Polyurethanes Chemistry and Technology. Part I. Chemistry*; John Wiley & Sons: New York, 1962; Vol. XVI.
(22) Heintz, A. M.; Duffy, D. J.; Hsu, S. L.; Suen, W.; Chu, W.; Paul, C. W. *Macromolecules* **2003**, *36*, 2695.
(23) Lide, D. R., Ed. *Handbook of Chemistry and Physics*, 80th ed.; CRC Press: Boca Raton, FL, 1999.
(24) Aylwin, P. A.; Boyd, R. H. *Polymer* **1984**, *25*, 323.

MA0474933